

# Innovations in image-guided radiotherapy

Dirk Verellen, Mark De Ridder, Nadine Linthout, Koen Tournel, Guy Soete and Guy Storme

**Abstract** | The limited ability to control for the location of a tumour compromises the accuracy with which radiation can be delivered to tumour-bearing tissue. The resultant requirement for larger treatment volumes to accommodate target uncertainty restricts the radiation dose because more surrounding normal tissue is exposed. With image-guided radiotherapy (IGRT) these volumes can be optimized and tumoricidal doses can be delivered, achieving maximal tumour control with minimal complications. Moreover, with the ability of high-precision dose delivery and real-time knowledge of the target volume location, IGRT has initiated the exploration of new indications for radiotherapy, some of which were previously considered infeasible.

## Gross tumour volume

The gross palpable or visible/ demonstrable extent and location of malignant growth.

## Clinical target volume

A tissue volume that contains the gross tumour volume and/ or subclinical malignant disease, which is to be eliminated. This volume has to be treated adequately in order to achieve the aim of radiotherapy: cure or palliation.

## Planning target volume

An additional margin added to the CTV that is a statistical construct to ensure that the desired dose can be anatomically realized in the CTV during treatment.

The probability of controlling a tumour through radiotherapy is proportional to the dose of radiation that is delivered, which is traditionally explained in a linear–quadratic model of cell killing<sup>1</sup>. The limiting factor in escalating the radiation dose to tumoricidal levels is the damage caused to nearby organs. In addition to dose tolerance, the irradiated volume of normal tissue is a crucial parameter in the development of radiation-induced toxicity. Traditionally, the irradiated volume encompasses the gross tumour volume (GTV) and the area at risk for microscopic spread. To assure a proper coverage of this clinical target volume (CTV), a margin is added to compensate for daily positioning errors and internal motion of organs, resulting in the planning target volume (PTV), to which the radiation dose is prescribed<sup>2,3</sup>. One way to increase the therapeutic dose to the tumour without increasing the irradiated volume of nearby tissues is to create a conformal dose distribution that tightly matches the shape of the target volume. This has become possible through the evolution of computerized planning systems and sophisticated dose-delivery systems. To further decrease the irradiated volume of nearby organs, it is necessary to decrease the PTV itself and thereby limit the volume of healthy tissue that is intentionally irradiated. The evolution of multimodality imaging has enabled the CTV to be more precisely delineated<sup>4–6</sup>, and such advances can affect treatment outcome<sup>7</sup>. These developments were recently reviewed by Bernier *et al.*<sup>8</sup>.

The introduction of image-guided radiotherapy (IGRT) has enabled knowledge of the exact position of the tumour and control of organ motion to be established

during treatment. As a result, the PTV margins can be substantially decreased (centimetres to millimetres), leading to a substantial reduction in the volume of radiation prescribed<sup>9–16</sup>. For example, reduction of a 2.0 cm to a 0.5 cm safety margin in a spherical tumour of 5 cm diameter results in a decrease in the irradiated volume of the surrounding organs from 316 cm<sup>3</sup> to 48 cm<sup>3</sup> (BOX 1). This Review highlights the recent progress in radiotherapy that has resulted from the synergistic combination of improved dose distributions — conformal radiotherapy (CRT) — and frequent imaging in the treatment room during a course of radiotherapy. As progress in CRT and IGRT were simultaneously implemented in the clinic, it is difficult to discriminate the relative contribution of each modality, so in this Review they will be discussed together. Decisions made on the basis of IGRT have drastically improved the quality of radiotherapy, and have broadened its use. High precision radiotherapy is required in situations in which the dose that has to be delivered to a tumour exceeds the tolerance dose of the surrounding tissues.

## Clinical considerations for IGRT

The therapeutic success of a radiation treatment is determined by the balance between tumour control probability (TCP) and normal-tissue complication probability (NTCP) — the TCP–NTCP balance. Indeed, in a high proportion of patients the biological dose necessary for tumour eradication can not be delivered because of a high probability of complications caused by collateral damage to nearby tissues. The principal goal of radiation research is to improve the TCP–NTCP balance. This might be achieved

UZ Brussel, Oncologisch Centrum, Radiotherapie, Laarbeeklaan 101, B-1090 Brussels, Belgium.  
Correspondence to D.V.  
e-mail: [dirk.verellen@uzbrussel.be](mailto:dirk.verellen@uzbrussel.be)  
doi:10.1038/nrc2288

**At a glance**

- In order to assure proper coverage of the clinical target volume (CTV) by radiation, a margin needs to be added to compensate for daily positioning errors and internal motion of organs, resulting in the planning target volume (PTV). The PTV therefore includes normal tissues near the tumour, to which radiation is intentionally delivered.
- The dose of radiotherapy that is necessary to control a tumour is often not delivered because of a high probability of complications in nearby normal tissues. This problem can be tackled by the generation of conformal dose distributions that tightly match the volume of the PTV and/or by decreasing the amount of normal tissue in the PTV.
- Image-guided radiotherapy (IGRT) is defined as frequent imaging in the treatment room that allows treatment decisions to be made on the basis of these images. IGRT aims at decreasing CTV-to-PTV margins from centimetres to millimetres.
- The synergy between conformal radiotherapy (CRT) and IGRT has drastically improved the quality of radiotherapy and has broadened its possibilities and indications. Clinical implementations of CRT-IGRT have enabled dose escalation, conformal sparing and non-uniform dose distributions, and initiated a revision of fractionation schedules.
- Research to improve image quality in radiotherapy is not new, but developments of software to quantify target localization errors, on the basis of in-room imaging and hardware allowing automated set-up, have stimulated mainstream clinical application of IGRT.
- IGRT makes use of many different imaging techniques, using modalities ranging from planar imaging to fluoroscopy to cone-beam CT, and following procedures as simple as using a single set-up image or as complex as intra-fraction tumour tracking.
- IGRT can be applied for managing of inter-fraction as well as intra-fraction geometric set-up uncertainties and for adapting treatments to tumour responses.

**Image-guided radiotherapy**

Frequent imaging in the treatment room during a course of radiotherapy to guide the treatment process.

**Conformal radiotherapy**

Describes the aim in radiotherapy of conforming or shaping the high-dose volume to the planning treatment volume. Alternatively, conformal avoidance refers to sparing of organs at risk.

**Normal-tissue complication probability**

With the introduction of 3D treatment planning systems, it has become possible to calculate and evaluate the dose distribution not only in tumours but also in nearby normal tissues. From these 3D dose distributions it is possible to model the outcome in biological terms of tumour control probability and normal-tissue complication probability. However, proper clinical validation of these models is still lacking.

by combining radiotherapy with chemotherapy, given the synergistic anti-tumoural effects of both modalities. Randomized trials in various solid tumours have demonstrated that combined modality treatment improves local control and overall survival, but significantly increases toxicity as well, which can be explained by a lack of discrimination in both radiotherapy and chemotherapy between cancer cells and rapidly dividing normal cells<sup>17–19</sup>. Modern radiosensitizing strategies try to exploit the biological specificity of tumours by targeting growth-factor and pro-angiogenic pathways such as epidermal growth factor (EGF) and vascular endothelial growth factor (VEGF), or by targeting specific features of the tumour microenvironment such as hypoxia or the pro-inflammatory tumour infiltrate<sup>20–26</sup>. Ongoing trials are evaluating whether the use of CRT-IGRT might decrease the NTCP of combined chemoradiotherapy. Unfortunately, herein lies one of the main frustrations of the discipline as developments have been introduced gradually, hampering randomized trials that would provide evidence-based benefit through clinically relevant end-points such as overall survival. However, recent phase I/II studies have already shown that the introduction of new technologies reduces complications and has paved the way for more aggressive treatment schedules (see below).

**Rationale for CRT-IGRT.** Recent developments in CRT-IGRT offer alternative strategies to improve the TCP-NTCP balance. New delivery techniques, such as intensity-modulated radiotherapy (IMRT), enable complex dose distributions with sharp dose gradients to be delivered, and this allows the

radiation dose to the target volume to be increased without increasing the irradiation of nearby tissues<sup>27</sup>. However, it is widely recognized that there are unavoidable uncertainties in the process of planning and delivering radiotherapy. Some of these relate to assessing the extent of microscopic disease spread, and others are associated with the delivery of the radiation itself. It is important that the magnitudes of these uncertainties are well understood and minimized whenever feasible, and that the possible influence on the outcome of treatment is estimated correctly. In conventional radiotherapy, information about the extent and frequency of these uncertainties is crucial in determining the safety margin around the tumour that is necessary to ensure ‘adequate’ tumour coverage, and in assessing whether the goal of sparing a critical organ is likely to be achieved. With the introduction of IMRT, exact knowledge and adjustment of appropriate margins becomes of primary importance, since the resulting sharp dose gradients are unforgiving with respect to misalignment and motion, as they can result in unacceptable high doses to healthy tissue or important under-dosage of the target volume. Nowadays, IGRT serves several purposes: first, reducing the treatment margins to an optimum level; second, providing an exact knowledge of anatomy during dose delivery in real time, which is required for ‘dose painting by numbers’ and hypofractionated radiotherapy; and third, the interactive adaptation of the treatment on the basis of daily assessment of changes in tumour volume and response to therapy (FIGS 1,2).

**Implementation of CRT-IGRT.** The first implementation of CRT-IGRT was in dose-escalation protocols in prostate cancer, and this resulted in improved biochemical control rates and prevention of an increase in rectal and bladder complications<sup>28,29</sup>. A retrospective analysis of 2,991 patients who were consecutively treated was reported by Kupelian and colleagues and showed equal biochemical failure rates for prostatectomy, permanent seed implantation and high-dose radiotherapy (> 72 Gray (Gy)), whereas the outcome was significantly worse for standard-dose radiotherapy (< 72 Gy)<sup>30</sup>. This study nicely illustrated that with the ability of CRT-IGRT to deliver higher doses, radiotherapy becomes an alternative to surgery. However, prospective randomized trials directly comparing radiotherapy with surgery are difficult to realize as most physicians and patients have a preference for one or other treatment modality, on the basis of local expertise and the availability or unavailability of CRT-IGRT.

As an alternative, the use of CRT-IGRT to spare normal tissues and maintain the dose to the target volume was successfully implemented in the treatment of head-and-neck cancer. The sparing of the parotid glands has decreased the incidence of xerostomia (dry mouth)<sup>31</sup>, improving patient quality of life. CRT-IGRT has also been used in the preoperative treatment of rectal cancer, in which helical tomotherapy (see below) has decreased the incidence of acute gastrointestinal and urinary toxicity<sup>32</sup>. Because intra-abdominal organs such as the small bowel, the stomach, the liver and the kidneys are more radiosensitive than most solid tumours, radiotherapy is

## Box 1 | Influence of margins on volume

The emphasis on improving dose distributions in radiotherapy is that as the treatment volume is reduced towards the target volume there is an increase in tolerance. As tolerance is increased, the dose to the target tissues can be raised. As the dose to the target tissues is raised, there will be higher tumour control probability. As treatment volume is reduced, there will, accordingly, be less irradiation of normal tissue and, therefore, a lower normal-tissue complication probability. The main cause of treatment-related morbidity is radiation damage to non-target tissue. The dose-volume effect is an important factor in this deduction and it might be interesting to draw attention to the third-power relationship between the radius (margins are generally expressed in one dimension) of a sphere and its volume ( $4/3 r \pi^3$ ), which is illustrated in the figure of the orange, in that a small reduction in margin (5mm) yields a reduction by half in volume (that is, the volume of the outer layer equals the volume of the core of the orange).

**Intensity-modulated radiotherapy**

Radiotherapy technique in which the intensity of irradiation varies within a radiation field. This can be obtained by using differential dose absorbers or by varying the time of radiation at different points.

**Dose painting by numbers**

Experimental intensity-modulated radiotherapy strategy in which the intensity of radiation intentionally varies within a tumour, on the basis of estimated levels of radioresistance that were assessed by biological and physical imaging modalities.

**Permanent seed implantation**

Radiotherapy in which the radiation source is implanted into the tumour (also known as brachytherapy). Prostate brachytherapy can deliver high and concentrated doses of radiation to the prostate gland.

**Tomotherapy**

A specially designed collimator generates an intensity-modulated profile and at the same time the gantry rotates about the long axis of the patient and as such irradiates a slice of the patient. One approach is the slice-by-slice arc rotation approach, in which the patient is translated longitudinally between consecutive gantry rotations to treat sequential transaxial slices. In the other approach, helical tomotherapy, the patient is being translated longitudinally, slowly and continuously, during the gantry rotation.

**Computed tomography**

In radiotherapy, volumetric IGRT solutions can be based on conventional kV X-ray sources or high energy MV photon beams that are used for treatment.

not commonly used for intra-abdominal malignancies<sup>33</sup>. In these cases as well, CRT-IGRT offers the possibility of prescribing tumoricidal radiation doses, while limiting the irradiated volume of these organs, and suggests a new therapeutic possibility for various gastro-intestinal cancers such as hepatic malignancies and pancreatic cancer.

**Biologically relevant dose optimization.** In conventional radiotherapy, a homogenous or uniform dose is generally delivered to the target volume without violating the tolerance of the nearby tissues. However, biologically it makes more sense to prescribe non-uniform target dose distributions. Models suggest that a significant increase in TCP might be gained from partial tumour boost doses, if they are delivered to 60% or more of the tumour volume<sup>34,35</sup>. Theoretically, this approach can decrease the local recurrence rate by enabling a large volume of the tumour to receive a lethal dose, and preventing repopulation of the boost volume by tumour cells. The concept of partial tumour boosts was developed many years ago and there is now renewed interest in this concept as the combination of IMRT and IGRT is enabling its clinical implementation. In addition, recent progress in biological and physical imaging modalities such as positron emission tomography (PET), single photon emission computed tomography (SPECT), dynamic contrast-enhanced magnetic resonance imaging (MRI) and magnetic resonance spectroscopy (MRS) can provide spatial information on the biological and physical characteristics of the tumour that might identify different levels of radioresistance<sup>36</sup>. This can be integrated technically into the treatment planning procedure, allowing biologically relevant dose optimization that takes into account estimations of hypoxia, cell proliferation rate and cell density<sup>37</sup>. The technique of applying non-uniform dose prescriptions is called voxel-intensity-based IMRT or dose painting by numbers. The intensity of the radiation varies from voxel to voxel according to the estimated level of radioresistance, as assessed by biological imaging. This strategy is currently being explored in experimental models and early clinical trials<sup>38–40</sup>.

Finally, the ability of high-precision dose delivery is initiating a revision of generally accepted fractionation schemes and concepts in radiobiology. Conventional radiation schedules with curative intention consist of 25–35 daily fractions of 1.8–2.0 Gy. Dividing the radiation dose into so many relatively small fractions decreases NTCP because of sublethal damage repair between dose fractions and cellular repopulation. Conversely, fractionation increases TCP because of reoxygenation of tumours and reassortment of cancer cells into radiosensitive phases of the cell cycle. However, these conventional fractionation schedules are often a burden for patients as they require daily visits to the hospital for 5–7 weeks and considerable machine time, which is an important factor in the economics of radiotherapy. These considerations led to the development of hypofractionated radiotherapy, which, by definition, uses fraction doses of more than 2 Gy. Hypofractionation was introduced in the clinic in the early 1960s for the treatment of breast cancer, where 3-day and 5-day treatment-per-week regimens were compared<sup>41</sup>. This and other studies showed that fraction sizes of more than 2 Gy produce significantly more unfavourable sequelae compared with conventional fractionation. Therefore, higher fraction doses were abandoned for the next 30–40 years to limit NTCP biologically<sup>42</sup>. As the introduction of CRT-IGRT offers a physical way to spare nearby tissues, the concept of hypofractionation is currently being revisited. If larger radiation fractions are given daily, it results in an acceleration of the treatment (therefore reducing overall treatment time), which reduces repopulation of rapidly proliferating tumours and increases TCP<sup>43</sup>. The recent evolution in IGRT has driven the development of stereotactic body radiotherapy (SBRT), an extreme form of hypofractionation that delivers an ablative dose of radiation in few fractions, which can disrupt tumour mitosis and other cellular functions. Several phase I/II studies have reported high levels of local control in lung cancer and liver metastasis, with acceptable toxicity<sup>44–46</sup>. Randomized trials that compare SBRT with surgery will soon be initiated.

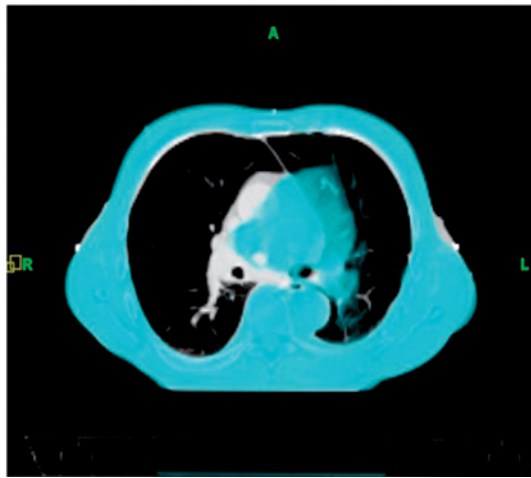


**Figure 1 | Megavolt computed tomography imaging.** Illustration of daily Megavolt computed tomography (MVCT) imaging (blue) acquired at the helical tomotherapy machine (TomoTherapy Inc.) superimposed on the reference kVCT data set (grey) showing a large deformation in the patient's anatomy due to a bronchial obstruction. This illustration clearly demonstrates the need for daily verification before treatment.

**Treatment simulator**

The treatment simulator is a machine that emulates the geometry of the treatment unit, but uses diagnostic quality X-rays to carry out localization and verification of the patient in treatment position.

**Linear accelerator**

A device that uses high frequency electromagnetic waves to accelerate charged particles such as electrons to high energies through a linear tube. The high-energy electron beam itself can be used for treating superficial tumours or it can be made to strike a target to produce high-energy (MV) X-rays for treating deep-seated tumours.

**Image registration**

The process of registering different image sets of the same modality (for example, CT-CT) or different modalities (for example, CT-MRI or CT-PET). This registration can be affine (that is, one set is translated, rotated or rescaled to match with the primary set assuming the patient's anatomy was not deformed) or deformable (that is, the registration algorithm deforms the secondary set to cope with internal and external deformations of anatomy).

**Electronic portal imaging device**

A device that enables automated acquisition of images acquired with a treatment beam.

**History of image-guidance in radiotherapy**

The history of radiation oncology follows an evolutionary path in that the most adapted technology survives, driven by the willingness to improve health care and provide optimal treatment quality for every patient. When reviewing literature it becomes clear that although without doubt some kind of IGRT must have been developed in the early days of kV-therapy (and later on with the use of high energy photons), the culture of IGRT was non-existent until the final decades of the last century. Patient set-up and the determination of treatment beams was in those days mainly guided by using a treatment simulator and drawing skin marks on the patient's surface that were consequently used to position the patient with respect to the treatment machine. The emphasis of positioning accuracy was on immobilization and applying conservative margins to ensure coverage of the target volume, rather than on imaging. One of the early studies that systematically used radiographic film placed distal to the patient was conducted by Haus *et al.* using <sup>60</sup>Co-irradiation, and showed a reduction in error rates (an error was recorded if the shift exceeded 1 cm) from 36% to 15% with more frequent verification films<sup>47,48</sup>. One of the few studies that correlated 'daily imaging' with outcome was published in the Patterns of Care Study review of patients with Hodgkin disease treated with radiotherapy alone<sup>49</sup>. These investigators observed that 33% of patients whose treatment portals were 'inadequate' subsequently developed in-field or marginal recurrence. During this time imaging was used to verify immobilization techniques not as a positioning technique on its own because radiographic film imaging using high-energy photon beams had serious limitations, such as poor contrast, inconsistent quality and lack of immediate results<sup>50,51</sup>.

A few centres have reported developments to increase positional accuracy based on in-room image guidance, such as mounting X-ray tubes on <sup>60</sup>Co-treatment units<sup>52,53</sup> or integrating X-ray tubes into the treatment head of the linear accelerator (linac)<sup>54</sup>. However, such developments were isolated efforts and were not adopted as mainstream practice. A possible explanation could be that outweighing the need for improved image quality was the need to develop tools to perform a quantitative comparison with reference data that would enable accurate patient set-up. It is fair to say that both the availability of computers and software tools for image registration and automation, as well as the introduction of conformal therapy, created the ideal environment to re-initiate the investigation of in-room imaging for accurate patient set-up.

The first papers on daily verification of patient set-up (using IGRT) were initiated for treatments in which positioning was more stringent than those typically associated with photon beam therapy. Proton therapy is a case in point as patients were selected because of the close proximity of radiosensitive organs to the target volume and an imaging methodology was required that did not use the actual treatment beam. Verhey *et al.* reported a technique for pre-treatment verification of patient positioning using radiographs obtained from three X-ray tubes mounted inside the treatment room<sup>55</sup>. In response to the need for superior conformation capabilities in photon beam therapy, Leong *et al.* developed a system featuring fast and high-quality portal images during the delivery of radiation, based on a fluorescent screen and camera combination<sup>56</sup>. This was soon followed by reports of using these electronic portal imaging devices (EPID) for 'online' correction<sup>57,58</sup>; that is, positioning the patient before beam delivery on a day-to-day basis. As an alternative to this technology, a matrix ionization chamber approach had been proposed<sup>59,60</sup>; and more recently amorphous silicon (aSi) imaging systems have been introduced<sup>61</sup>. With the introduction of the online concept, the need for seamless integration and automation became apparent<sup>61,62</sup> and the possibility of 3D evaluation<sup>63</sup> as well as true 3D correction was introduced clinically<sup>64-68</sup>. So far, these developments have focused on inter-fraction set-up uncertainties assuming that the target volume remains relatively fixed in space during treatment. Recently the online concept has been taken one step further in that efforts to manage intra-fraction motion are being explored, either by tracking the target volume or gating the beam on the basis of image-guidance technology<sup>69-74</sup>. This development is related to similar developments in time-resolved or 4D diagnostic image acquisition that can describe internal motion of target volumes and organs at risk<sup>75,76</sup>. Finally, the idea of using imaging devices placed distal to the patient during treatment for evaluation of the exit dose is now a reality<sup>77-79</sup>, initiating new approaches such as adaptive radiotherapy in which the imaging technology is used to assess treatment response and refine the dose delivery accordingly on a day-to-day basis<sup>80,81</sup> (FIG. 2).

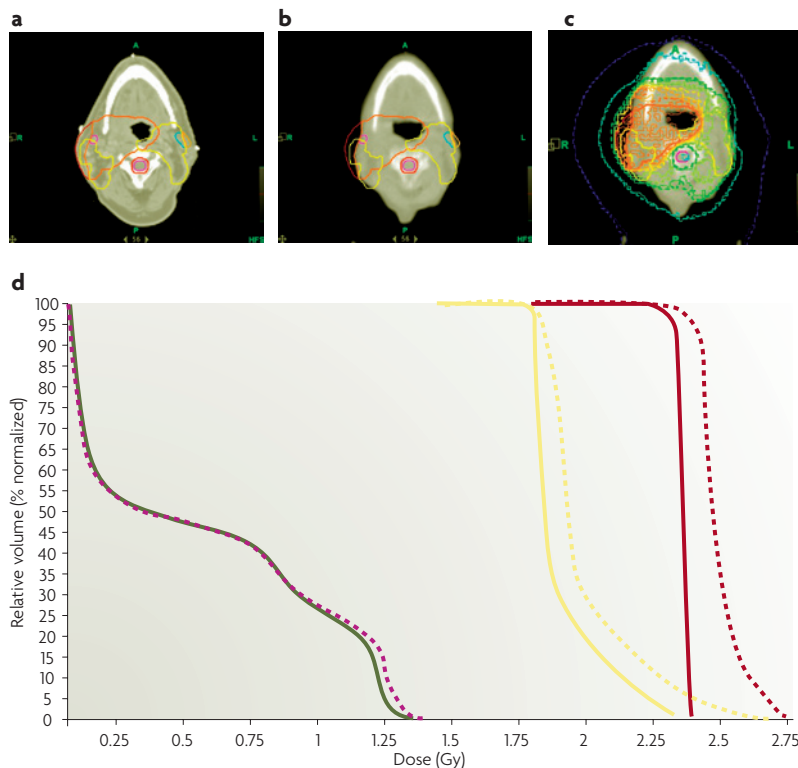


**Figure 2 | Adaptive radiotherapy.** An illustration of adaptive radiotherapy in which the MV computed tomography (MVCT) image taken at the end of a treatment course together with the actual treatment-delivery parameters of that day are used to recompute the dose distribution. Two of the top panels (**a**, **b**) show the original contours (planning target volume in red) superimposed on the original kVCT set (**a**) and the daily MVCT image (**b**); note the considerable shrinkage of the patient's outer contour. The other images (**c**, **d**) show a comparison of the original dose distribution (solid colour lines) with the actual delivered dose (dashed lines). This information can be summed for the entire treatment or at any time during the course of treatment to help decide whether or not it is advisable to adapt the treatment (for example, the green solid line and pink dashed line represent the original and present dose volume histogram (DVH) of the spinal cord, respectively).

### Image-guidance techniques

As this is a Review of IGRT, immobilization techniques and margin recipes will not be covered in detail. However, it is important to realize that to fulfil its full potential, IGRT will need to be combined optimally with both concepts: immobilization devices to help the patient maintain a certain position; and margins to counteract inter-observer variability in volume delineation, compensate for uncertainties in the involvement of disease, and represent the remaining geometric uncertainty. IGRT has shown that immobilization techniques on their own are no guarantee of high accuracy<sup>47,48,82–84</sup>. Accurate assessment of geometric errors, however, remains extremely important and emanates from the definition of margins. In the literature many different recipes have been proposed for margin generation based on different statistical methods<sup>9,13,85</sup>.

The clinical application of IGRT for patient set-up verification and correction can generally be classified as either an offline or an online patient set-up. The former monitors the position of the patient during a limited number of fractions and adapts the safety margins and/or

treatment plan accordingly; it is also known as adaptive radiotherapy (ART). The online approach offers the possibility of reducing most geometric errors (both systematic and random), but requires that the quantification and correction of target localization errors is automated to make it efficient to use in clinical routine. An extremely important feature of IGRT is the ability to register the daily images to a reference image set that has usually been generated at the time of treatment planning and represents the ideal situation (that is, perfect alignment of treatment beam and target volume). The purpose of image registration is to find the transformation (translation, rotation and preferably deformation) that maps one set onto the other to obtain the corresponding adjustments that are required to align target volume and treatment beam as accurately as possible. Coping with anatomical deformation, however, has proved challenging in patient set-up procedures<sup>86–88</sup>. Finally, it has to be noted that most IGRT approaches make use of imaging modalities that range from planar imaging to fluoroscopy to CT-based solutions, and follow regimens as simple as acquiring single set-up images or as complex as assessment of intra-fraction tumour tracking. This might have an important effect on the concomitant dose (both concentrated at the skin in the case of planar kV X-ray imaging or distributed throughout the anatomical volume of interest when CT-based imaging is introduced) that a patient receives. Indeed, the wide variety of modalities and the combination of added patient dose due to increased imaging in the preparation of treatment as well as changes in dose administration from recent developments in treatment delivery (for example, IMRT), make it difficult to synthesize a complete picture of the patient's exposure<sup>89</sup>.

### Peripheral solutions for IGRT

The concept of 'peripheral' in this classification refers to in-room imaging devices that are not directly mounted on the treatment machine. Being independent of the beam-delivery device, peripheral solutions to IGRT have the advantage that in principle they can be used to cope with organ motion and/or patient motion during irradiation (so called intra-fraction motion). In turn, this concept has a disadvantage in that the system needs to be carefully calibrated with respect to the isocentre of the machine and this introduces an additional source of uncertainty (BOX 2).

The combination of multiple X-ray source and detector systems has been introduced to solve the inherent 2D limitation in target localization of using Megavolt (MV) images generated with the high-energy treatment beam, such as portal films or EPIDs<sup>61</sup> (see below). The approach of using diagnostic X-rays for treatment set-up verification is not new<sup>52–55,90,91</sup> and offers a threefold advantage in that image quality (a well-documented problem in MV-based imaging) is no longer an issue, especially in combination with aSi detectors<sup>61,92</sup>, patient dose has become less important compared to daily MV imaging, and this modality can be used in fluoroscopic mode during treatment. The Mitsubishi Electronics Co. in collaboration with Hokkaido University have developed a room-mounted kV-imaging device<sup>70,71</sup>,

#### Offline patient set-up

The offline approach monitors the position of the patient during a limited number of fractions and adapts the safety margins accordingly. This approach does not allow for decreasing the treatment margins sufficiently for aggressive conformal radiotherapy.

#### Online patient set-up

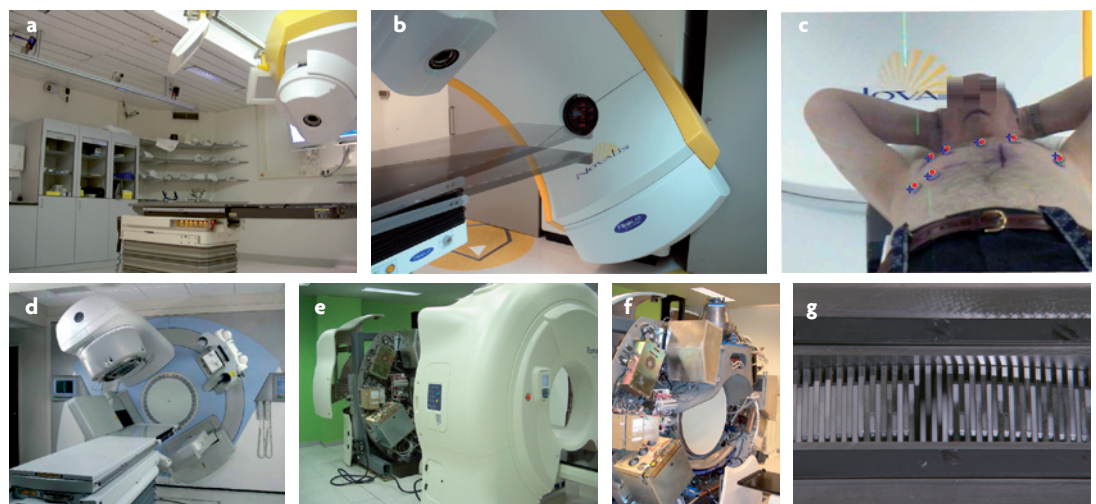
The online approach offers the possibility of reducing most geometric errors (both systematic and random), but is considered to be time consuming and requires automated control of the treatment couch to make it efficient in clinical practice.

Box 2 | Image-guidance technologies

Typical examples of the technological solutions are given. The examples given are not exclusive, but chosen to illustrate the concept.

The ExacTrac/NovalisBody system (BrainLAB AG) combines an infrared tracking system (note the infrared cameras mounted to the ceiling in (a) of reflective markers that are placed on the patient's surface allowing real-time monitoring of the patient's position in space and extraction of a respiratory signal (c), a pair of X-ray tube/detector imagers (two flat-panel detectors mounted to the ceiling — a — and two X-ray tubes embedded in the floor — b) to subtract 3D information of the patient's anatomy on the basis of bony structures or implanted radio-opaque markers and a robotic couch (b) to adjust translational and rotational set-up errors before treatment. The beam on-off signal of the linear accelerator (linac) can be triggered by the respiratory signal that is obtained from the real-time tracking of the infrared reflective markers.

An example of an X-ray tube/detector assembly mounted orthogonally to the treatment beam (d; courtesy of Elekta). The concept can be used for stereoscopic 2D–3D imaging in combination with the electronic portal imaging device system mounted in the treatment beam axis distal to the patient, or to generate a volumetric cone-beam computed tomography (CT) acquisition by rotating the gantry before treatment. Illustrated is the 'two-in-one' helical tomotherapy concept (TomoTherapy Inc.) with the 6MV linac (e) and binary collimating device (g) replacing the traditional X-ray tube from diagnostic CT scans, and the traditional detector array (f) for helical image acquisition.



soon to be followed by similar reports from the UZ Brussel in collaboration with BrainLAB AG on the ExacTrac/NovalisBody system, which uses a combination of infrared reflective markers and a robotic couch to accurately correct for both translational and rotational set-up errors<sup>64,65,67,68</sup>. However, some criticisms exist as the patients might involuntarily counteract the couch motion<sup>93</sup>.

Alternatively, the Cyberknife approach (Accuray Inc.) leaves the patient undisturbed by using a linac on a robotic arm with 6 degrees of freedom that enables the beam delivery device to be positioned according to the image information<sup>94</sup>. The combination of multiple planar (2D) images simultaneously acquired allows for 2D–3D registration of the patient's anatomy to the reference information subtracted from the treatment planning system. Room-mounted X-ray imaging systems are particularly suitable for tracking internal fiducial markers (such as implanted radio-opaque objects) during treatment<sup>70,71</sup>. The X-ray sources and imagers are fixed on either the floor or ceiling to provide high mechanical precision, provided that a proper calibration has been established. A major disadvantage of this solution is the inability to visualize soft tissue, meaning that surrogate structures (bony landmarks

or implanted radio-opaque markers) are required to acquire positional information of the target volume. Another drawback is the lack of information about the spatial relationship between the target and adjacent organs that are at risk during treatment.

Diagnostic CT scanners have been introduced in the treatment room because they have the advantage of not requiring a surrogate to visualize soft tissue targets. The scanner can be positioned over the treatment couch using rails and/or the treatment couch can be used to transport the patient into the bore of the CT gantry<sup>95–98</sup>. Another way to visualize soft tissue before treatment is ultrasound devices<sup>99,100</sup>. Unfortunately, these devices need an operator to be present during the investigation and therefore can not be used while the beam is on. Moreover, ultrasound-based positioning is limited to superficial and abdominal locations (typically prostate), and it has been argued that this solution is susceptible to inter-observer variations and the possible introduction of displacement owing to pressure of the imaging probe on the patient's lower abdomen<sup>101,102</sup>. Another method to localize the target volume non-radiographically in 3D is based on miniature implantable radiofrequency transponder coils<sup>103,104</sup> that can be tracked electromagnetically in real time from outside the patient.

**Peripheral solutions to IGRT**  
In-room imaging systems that are not mounted physically on the treatment-delivery system.

**Isocentre**  
The point of intersection of the central axis of the radiation beam and the horizontal axis of rotation of the gantry. Traditionally the centre of the planning treatment volume coincides with the isocentre.

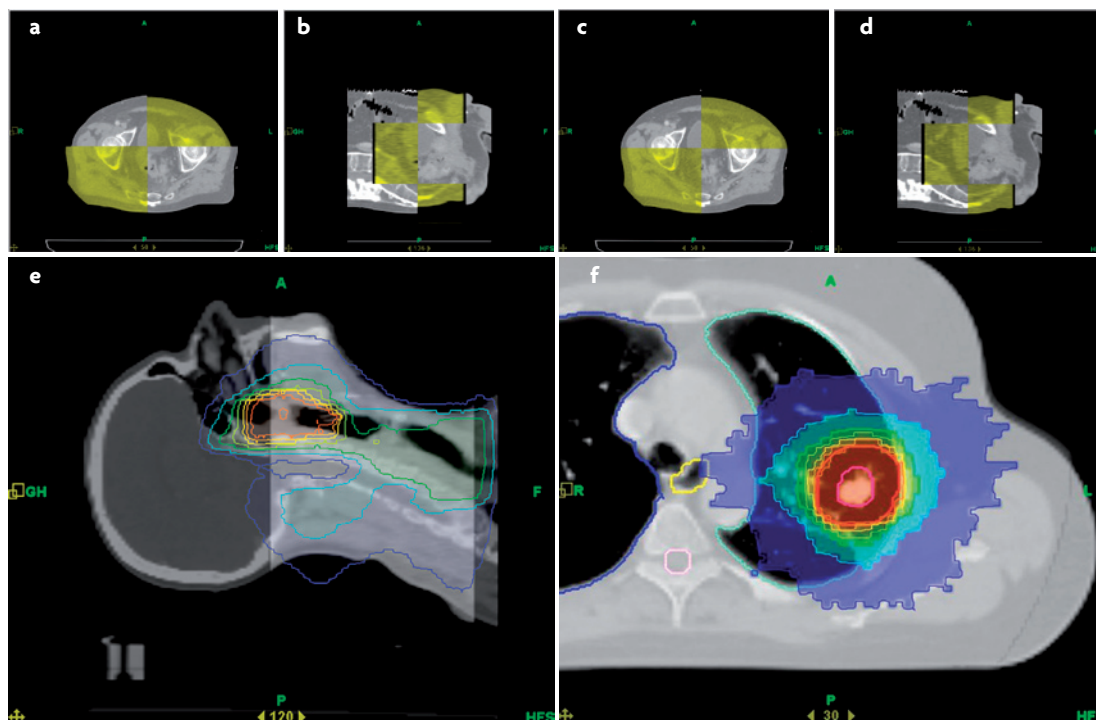


**Figure 3 | Combined computed tomography and daily MVCT image data.** Example of an overlay (axial and sagittal cross-sections are shown) of planning computed tomography data (grey) and daily Megavolt computed tomography (MVCT) data (yellow), prior to (a, b) and after (c, d) adjustment. The necessary adjustments required for registration of both imaging sets yield information on the corrections that are required for patient set-up. The planned dose distribution can also be superimposed on the daily MVCT image (TomoTherapy Inc.) to align the patient's anatomy with the dose distribution (e, f). In this illustration the dose distribution is colour coded from blue to red representing low to high dose, respectively. The daily MVCT image (light grey) is superimposed on the reference kVCT data (dark grey) and the dose distribution is used to align the spinal cord with the corresponding low-dose valley (e). A lung tumour is visible in the daily MVCT image and aligned with the dose distribution before treatment (f).

### On-board solutions

On-board solutions refer to imaging devices that are physically attached to the treatment delivery system. The most widespread on-board IGRT technology is the EPID that was first described by Leong *et al.*<sup>56</sup>, and a comprehensive overview can be found in the report of the American Association of Physicists in Medicine (AAPM) radiotherapy committee task group 58 (REF. 61). A major advantage of this approach is the use of the actual treatment beam to ensure alignment of beam and target (that is, replacing the conventional radiographic films or portals). In addition to this, the EPID can be used for dose measurements, which is extremely useful in detecting differences between actual patient data as encountered during treatment and those applied during treatment planning<sup>77,78</sup>. EPIDs are likely to become useful for quality assurance of the radiotherapy process. Being a planar (as opposed to volumetric) imaging device that is mounted on the treatment delivery system distal to the patient, it requires multiple gantry positions to obtain 3D information. The latter has been solved by introducing an additional X-ray source and detector system perpendicular to the treatment beam axis, or two additional gantry-mounted X-ray systems with central axes intersecting each other at the isocentre of the linac<sup>105</sup>. Moreover, both the EPID imager<sup>106</sup> and an orthogonally

mounted X-ray imaging device<sup>63</sup> can be used to acquire cone beam volumetric CT (CBCT) data. Jaffray *et al.* illustrated the volumetric nature of the CBCT data, showing excellent spatial resolution in all three dimensions (as opposed to conventional CT in which the cranio-caudal resolution depends on the slice thickness and pitch)<sup>63</sup>. In principle, these cone-beam-based solutions offer sufficient soft tissue visualization to avoid the need for surrogates in localizing most target volumes or critical structures. On the other hand, volumetric imaging while the beam is on is not possible and is limited to positioning the patient before treatment. The major weakness of the gantry-mounted systems is the sub-optimal mechanical precision (for example gantry sagging) and the scatter radiation from the patient to the imagers.

### Integrated solutions

It is difficult to make a clear classification of integrated solutions, as some features of the previous techniques, such as good image quality, software tools to obtain quantitative data for target localization, and automation of patient set-up, are seamlessly integrated into the treatment process. Some techniques have been added to existing equipment and adapted to an application that was not foreseen when the device was developed. An example is the EPID, which was originally designed for planar

#### On-Board IGRT system

In-room imaging systems that are physically attached to the treatment-delivery system.

#### Cone beam volumetric CT

A CT scanning method in which the fan-beam and linear detector array is replaced with an open-beam and large-area flat-panel detector to generate volumetric images through a single rotation of the system.

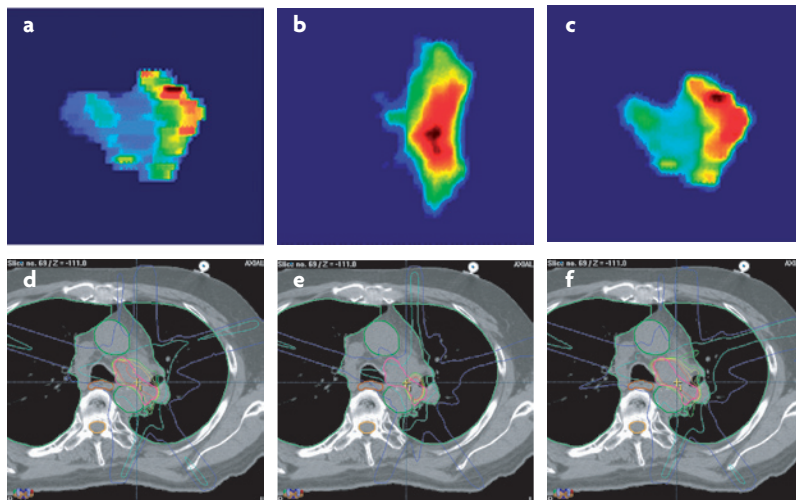


**Figure 4 | Intensity-modulated radiotherapy and motion.** Illustration of intensity-modulated radiotherapy fluence maps for one out of five beams used for a treatment of a tumour in the mediastinum (thorax) and the resulting dose distributions in an axial plane. From left to right: theoretical fluence map (a,d), fluence map obtained in motion (b, e) and fluence map in motion but acquired in respiration-gated mode (c,f). The dose distribution is colour coded from blue to red representing low to high dose, respectively. Note the substantial under-dosage due to motion in the central image.

field verification<sup>56</sup> but has been adapted for CBCT<sup>106</sup> and *in vivo* dosimetry<sup>77,78</sup>. However, as the system was not designed for that purpose, it features some major weaknesses such as mechanical instability and scatter issues that require corrections and post-processing. Although this approach of exploring alternative uses for established equipment might result in a sub-optimal solution, it can be considered to be proof of concept. Therefore, we use the term ‘integrated solution’ to refer to a concept that grew out of previous developments but was designed from the start for a certain purpose.

The helical tomotherapy (TomoTherapy Inc.) approach<sup>79,107,108</sup> is an example of this, in which the concept of an add-on sequential tomotherapy<sup>109–111</sup> device has been combined with helical CT-scanning to result in a two-in-one concept. It is a treatment modality in which IMRT is delivered in a rotational fashion using a 6 MV linac mounted to a ring-based gantry. Simultaneously, the patient is slowly translated through the bore allowing high modulation and conformity of the dose distribution. From the patient’s point of view the source describes a helical trajectory, hence its name. The continuously rotating gantry combined with a CT-detector array system allows MVCT imaging and can be used for *in vivo* dose-transmission measurements for dose verification. Basically it is a CT-scanner in which the diagnostic X-ray tube has been replaced with a 6 MV linac and the collimating jaws (or shutters) replaced with a binary collimator that consists of small high-density metal leaves, creating 64 small beams that can be switched on and off rapidly for IMRT by varying the fraction of opening time during rotation (BOX 2). In a way similar to diagnostic CT, the patient is treated in slices by a narrow photon beam. CT-image acquisition is accomplished with all leaves open before treatment

**Dose volume histogram**  
An alternative method for displaying the results of dose calculation. The histogram shows the percentage of the volume of any structure that is irradiated above a particular dose level. More correctly known as cumulative DVH.

**Multi-leaf collimator**  
Computers have enabled the replacement of field-shaping beam blocks, which create irregularly shaped irradiation fields to spare vulnerable tissues, with an MLC. MLCs consist of 40–120 movable leaves, with a width varying between 0.2 and 1.0 cm, that are arranged in opposed pairs.

(FIG. 3). As target volumes are treated in a slice-by-slice approach the efficiency of helical tomotherapy for moving targets can be questioned. Mitsubishi Heavy Industries Ltd., in collaboration with the University of Kyoto, recently developed another ring-based system with a linac-collimator assembly that allows pan and tilt motion to track the tumour on the basis of information from two sets of kV X-ray tubes and flat panel detectors also integrated into the gantry<sup>112</sup>. The imaging device can be used in fluoroscopic mode during treatment or for CBCT acquisition before treatment. In addition an EPID is integrated, which potentially allows for imaging and dose verification. As power connections and data communication is carried out with cables through an umbilicus-like connection, the system does not allow for continuous rotation and it has a limited field width of 14 × 14 cm<sup>2</sup>.

A logical next step is to introduce MRI in IGRT as it offers superior soft tissue contrast compared with radiographic imaging. At the University of Utrecht a prototype is being designed that combines a linac mounted on a ring-based gantry and a 1.5 Tesla MRI device<sup>113</sup>. The approach is inherently limited by interaction of the radio-frequency signal that is used for MRI with the radio-frequency pulses that are required for electron acceleration in the linac, and the influence of the strong magnetic field from the MRI on the dose-absorption process. To cope with these limitations, a 0.3 T MRI has been designed combined with three <sup>60</sup>Co-sources that are equipped with multi-leaf collimators (MLC) for IMRT mounted on a ring-based gantry (J. Dempsey, personal communication). Both MRI concepts are promising but are still in the development phase. A possible future development will be the introduction of PET to monitor the metabolic response of the target as well as the dose deposition during treatment<sup>114</sup>.

**Image-guidance and motion management**

Respiratory motion affects all tumour sites in the thorax and some in the abdominal region, and again, motion control will allow for reduction of irradiated healthy tissues and possible escalation of dose to the target volume<sup>115</sup>. Apart from techniques to accurately describe motion, different methods are being developed for motion management during treatment, such as forced shallow breathing by abdominal compression<sup>83,116</sup> or breath hold<sup>117,118</sup>, motion-encompassing techniques<sup>119</sup>, and breathing synchronized techniques such as respiratory gating<sup>70,71,73,74,120</sup> and real-time tracking<sup>69,94,121</sup>. All these techniques require some kind of IGRT to reach full potential. Using a stereotactic body frame<sup>116</sup> to suppress breathing-induced motion, Wulf *et al.* showed that with a margin for target variability of 5 mm (antero-posterior and latero-lateral) and 10 mm (cranio-caudal) about 12–16% of the targets might be partially missed<sup>83</sup>. Therefore, the conclusion was drawn to recommend CT verification before each treatment session to detect these targets with increased reproducibility. Motion-encompassing techniques refer to the idea of incorporating information on tumour motion into the treatment planning process, either by introducing

patient-individualized margins or using this information in the optimization procedure<sup>122–124</sup>. Internal motion can be assessed by time-resolved imaging techniques such as ‘slow’ CT scanning or PET, which owing to its slow acquisition time offers information on tumour position probability<sup>119,125–127</sup>. Alternatively, multiple fast CT acquisitions during the respiratory cycle can be used to describe the motion of the target during the respiratory cycle. However, respiratory motion is irregular and there are no general respiratory patterns that can be assumed by observation before treatment.

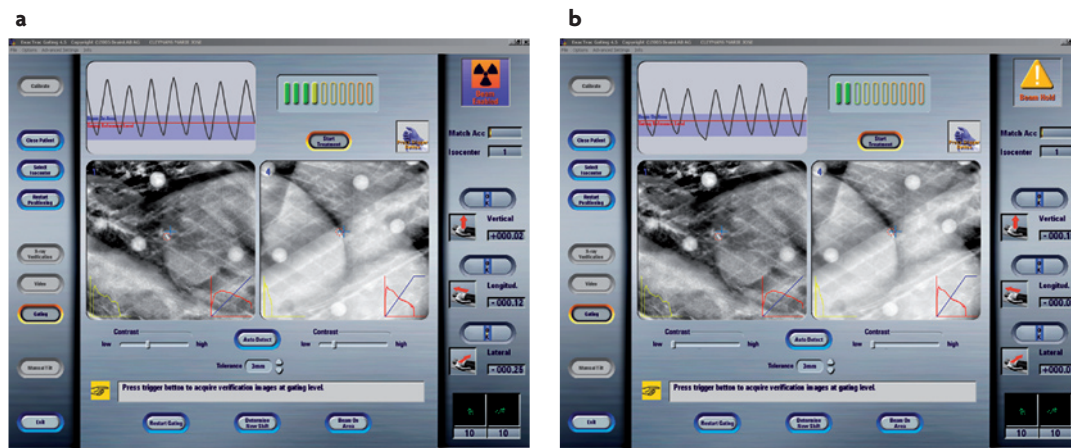
Organ motion causes an averaging or blurring of the static dose distribution along the path of motion, and for IMRT an additional motion artefact follows from a possible interplay between motion of the leaves of the collimator and the component of target motion that is perpendicular to the beam<sup>66,73,74,123,128</sup> (FIG. 4). As a result, respiratory-synchronized techniques will most often offer the optimal solution. It should be noted that the object being measured for motion could be the tumour itself, an artificial marker implanted in or near the tumour<sup>70,129,130</sup> or a surrogate organ such as the diaphragm<sup>118,131</sup>. Moreover, the breathing pattern itself is usually obtained from an external signal, which allows real-time observation (for example, infrared reflective markers placed on the patient’s surface, spirometers or a flexible bellow), and the mechanical coupling with the tumour is often weak, which results in complex relationships. Based on 4D CT measurements, Lu *et al.* have shown that the relationship to internal motion is strongest with the amplitude of the external signal (the

signal for respiratory motion can be characterized by amplitude or phase)<sup>75</sup>. However, the correlation between breathing pattern and tumour position can be disturbed or lost completely by transient changes in breathing. Breathing-synchronized techniques need to establish a correlation between the real-time external breathing signal and the internal tumour motion, and this correlation needs to be verified at regular intervals during the course of treatment.

Respiratory gating involves the administration of radiation at certain intervals within a particular portion of the patient’s breathing cycle, commonly referred to as the ‘gate’ (BOX 3). The choice of gate width is a trade-off between minimizing motion within the gate and the amount of time that the beam is on, and breath-hold techniques are being introduced to optimize the duty cycle<sup>117</sup>. Some studies have shown the anatomical position of the tumour to be more reproducible at end respiration<sup>131</sup>. On the other hand, when breath-hold techniques are introduced at (moderate) deep inspiration the relative damage to healthy lung tissue can be reduced and it seems to be more comfortable for the patient<sup>117,132</sup>. Another means of accommodating respiratory motion is to reposition the radiation beam dynamically so as to follow the changing position of the tumour; this is referred to as real-time tumour tracking and can be established by synchronizing the collimating system of the linac with the target motion<sup>121</sup>. With conventional multi-leaf collimators, only one dimension can be compensated for efficiently and the beam-collimating device needs to be aligned such that the leaf

### Box 3 | Breathing-synchronized irradiation

Breathing-synchronized irradiation requires a technology to monitor the breathing motion and its relationship with the actual tumour position. Consequently, this information is used to trigger the treatment beam. In this illustration, the respiratory signal was obtained with infrared markers attached to the patient’s skin, whereas the tumour was localized with an implanted radio-opaque marker. The two panels shown (a, b) were acquired with the peripheral dual X-ray source/detector system from BrainLAB (BOX 2); in the left upper corner the patient’s respiratory signal is shown, which when it coincides with the treatment window or ‘gate’ (purple shaded area) triggers the beam for treatment (a), and when this signal leaves this gate the beam will be shut off (b). As the relation between external breathing signal and tumour motion can change during treatment, this relationship needs to be verified constantly during treatment and multiple images are acquired on a regular basis at the reference level (red line inside the gate). In this case a tolerance sphere has been defined with 3 mm diameter (red/white circles in the images). If the projection of the radio-opaque implanted marker coincides with the sphere, treatment will continue, otherwise an interruption will occur and the correlation needs to be re-established.



motion coincides with the major axis of the tumour motion. Compensation of 2D motion might be achievable with the pan-and-tilt-like solution currently under development<sup>112</sup>. Full 3D compensation is realized with the linac mounted to a robotic arm<sup>69,72,94,130</sup>. Compared with the gating technique the tracking approach potentially offers higher delivery efficiency and less residual target motion provided there is no system latency in the beam adaptation<sup>130</sup>. It should be noted that these tracking approaches rely on an accurate prediction model of the breathing motion to anticipate the future position of the tumour, and this has proved to be challenging<sup>133</sup>. Again, breath-hold techniques have been introduced, this time to avoid a possible systematic lag in the tracking procedure. An excellent overview of the management of respiratory motion in radiotherapy is given by the AAPM Task Group 76 (REF. 134).

**Conclusion**

Over the past 50–60 years treatment volumes have been reduced stepwise and with success: kV X-ray treatment units were replaced by <sup>60</sup>Co units and then linear accelerators; large rectangular fields were replaced by smaller fields shaped to accord with the particular features of the individual patient; conformity increased with IMRT; and delivering simultaneous integrated boost and non-uniform dose distributions became realistic. These technical developments have been implemented successfully in the clinic because of a greater ability to define the target tissues and confirm that these tissues were indeed covered by the beam. Initially, attempts

to verify beam alignment with target volume were limited by the poor quality and cumbersome use of radiographic films. The introduction of EPIDs initiated the possibility of automation, which could be seen as a revolution comparable to the introduction of CT in the planning process. This concept is currently evolving into 3D volumetric imaging, and correcting and real-time (4D) motion management. Real-time dose assessment enables the adapting or refining of the treatment according to the response before treatment on a day-to-day basis. IGRT can monitor daily organ movement, tumour shrinkage during the course of treatment and in-patient dosimetry. These developments, in turn, have allowed dose painting by numbers, revision of dose fractionation schedules and exploring new indications in radiotherapy.

It has been said that surgery and perhaps radiotherapy have reached their maximum effectiveness, but failure to control the primary tumour and its regional spread is no less a problem today than when it was first quantified by Suit in 1970 (REF. 135). IGRT seems certain to eliminate obstacles that have hindered the ability to use both higher doses and tighter margins around the tumour. With CRT-IGRT, not only will we tailor doses within and around the tumour, but IGRT gives us the confidence fraction-to-fraction or even during dose delivery that variations in patient set-up and organ motion are dealt with, and we can start treating the moving, breathing patient adequately. The main clinical benefit without doubt will be a reduction of toxicity and increased quality of life for the patient.

1. Brenner, D. J., Hlatky, L. R., Hahnfeldt, P. J., Huang, Y. & Sachs, R. K. The linear-quadratic model and most other common radiobiological models result in similar predictions of time-dose relationships. *Radiat. Res.* **150**, 83–91 (1998).
2. International Commission on Radiation Units and Measurements. *Prescribing, Recording and Reporting Photon Beam Therapy, Report 50* (ICRU, Bethesda, 1993).
3. International Commission on Radiation Units and Measurements. *Prescribing, Recording and Reporting Photon Beam Therapy, Report 62* (ICRU, Bethesda, 1999).  
**References 2 and 3 describe the rationale behind the concept of treatment margins in radiotherapy and provide a clear definition of the different volumes.**
4. Wang, D. *et al.* Initial experience of FDG-PET/CT guided IMRT of head-and-neck carcinoma. *Int. J. Radiat. Oncol. Biol. Phys.* **65**, 143–151 (2006).
5. Balter, J. M. & Kessler, M. L. Imaging and alignment for image-guided radiation therapy. *J. Clin. Oncol.* **25**, 931–937 (2007).  
**This review explores the issues surrounding the use of images and image registration for treatment planning and treatment verification in radiotherapy.**
6. Gregoire, V. Is there any future in radiotherapy planning without the use of PET: unraveling the myth. *Radiother. Oncol.* **73**, 261–263 (2004).
7. Rothschild, S. *et al.* PET/CT staging followed by Intensity-Modulated Radiotherapy (IMRT) improves treatment outcome of locally advanced pharyngeal carcinoma: a matched-pair comparison. *Radiat. Oncol.* **2**, 22 (2007).
8. Bernier, J., Hall, E. J. & Giaccia, A. Radiation oncology: a century of achievements. *Nature Rev. Cancer* **4**, 737–747 (2004).  
**In this excellent review Bernier and colleagues highlight the progress of radiation therapy in the twentieth century with emphasis on the refinements of irradiation techniques and radiobiology. This Review and Bernier's review are complementary.**
9. Bel, A., Van Herk, M. & Lebesque, J. V. Target margins for random geometrical treatment uncertainties in conformal radiotherapy. *Med. Phys.* **23**, 1537–1545 (1996).
10. Bel, A. *et al.* High-precision prostate cancer irradiation by clinical application of an offline patient setup verification procedure, using portal imaging. *Int. J. Radiat. Oncol. Biol. Phys.* **35**, 321–332 (1996).
11. Van Herk, M. *et al.* Quantification of organ motion during conformal radiotherapy of the prostate by three dimensional image registration. *Int. J. Radiat. Oncol. Biol. Phys.* **33**, 1311–1320 (1995).
12. Yan, D., Wong, J. W., Gustafson, G. & Martinez, A. A new model for 'accept or reject' strategies in off-line and on-line megavoltage treatment evaluation. *Int. J. Radiat. Oncol. Biol. Phys.* **31**, 943–952 (1995).
13. Yan, D. *et al.* Adaptive modification of treatment planning to minimize the deleterious effects of treatment setup errors. *Int. J. Radiat. Oncol. Biol. Phys.* **38**, 197–206 (1997).
14. Alasti, H., Petric, M. P., Catton, C. N. & Warde, P. R. Portal imaging for evaluation of daily on-line setup errors and off-line organ motion during conformal irradiation of carcinoma of the prostate. *Int. J. Radiat. Oncol. Biol. Phys.* **49**, 869–884 (2001).
15. De Neve, W. *et al.* Interactive use of on-line portal imaging in pelvic radiation. *Int. J. Radiat. Oncol. Biol. Phys.* **25**, 517–524 (1993).
16. Gildersleve, J. *et al.* A randomised trial of patient repositioning during radiotherapy using a megavoltage imaging system. *Radiother. Oncol.* **31**, 161–168 (1994).
17. Schaake-Koning, C. *et al.* Effects of concomitant cisplatin and radiotherapy on inoperable non-small-cell lung cancer. *N. Engl. J. Med.* **326**, 524–530 (1992).
18. Herskovic, A. *et al.* Combined chemotherapy and radiotherapy compared with radiotherapy alone in patients with cancer of the esophagus. *N. Engl. J. Med.* **326**, 1593–1598 (1992).
19. Krook, J. E. *et al.* Effective surgical adjuvant therapy for high-risk rectal carcinoma. *N. Engl. J. Med.* **324**, 709–715 (1991).
20. De Ridder, M. *et al.* Lipid A radiosensitizes hypoxic EMT-6 tumor cells: role of the NF-kappaB signaling pathway. *Int. J. Radiat. Oncol. Biol. Phys.* **57**, 779–786 (2003).
21. Brown, J. M. & Wilson, W. R. Exploiting tumour hypoxia in cancer treatment. *Nature Rev. Cancer* **4**, 437–447 (2004).
22. De Ridder, M. *et al.* Macrophages enhance the radiosensitizing activity of lipid A: a novel role for immune cells in tumor cell radioresponse. *Int. J. Radiat. Oncol. Biol. Phys.* **60**, 598–606 (2004).
23. Bonner, J. A. *et al.* Radiotherapy plus cetuximab for squamous-cell carcinoma of the head and neck. *N. Engl. J. Med.* **354**, 567–578 (2006).
24. De Ridder, M. *et al.* The radiosensitizing effect of immunoadjuvant OM-174 requires cooperation between immune and tumor cells through interferon-gamma and inducible nitric oxide synthase. *Int. J. Radiat. Oncol. Biol. Phys.* **66**, 1473–1480 (2006).
25. Nyati, M. K., Morgan, M. A., Feng, F. Y. & Lawrence, T. S. Integration of EGFR inhibitors with radiochemotherapy. *Nature Rev. Cancer* **6**, 876–885 (2006).
26. Czito, B. G. *et al.* Bevacizumab, oxaliplatin, and capecitabine with radiation therapy in rectal cancer: Phase I trial results. *Int. J. Radiat. Oncol. Biol. Phys.* **68**, 472–478 (2007).
27. Intensity Modulated Radiation Therapy Collaborative Working Group. Intensity-modulated radiotherapy: current status and issues of interest. *Int. J. Radiat. Oncol. Biol. Phys.* **51**, 880–914 (2001).  
**A critical review describing the state-of-the-art in IMRT in 2001.**
28. Peeters, S. T. *et al.* Dose-response in radiotherapy for localized prostate cancer: results of the Dutch multicenter randomized phase III trial comparing 68 Gy of radiotherapy with 78 Gy. *J. Clin. Oncol.* **24**, 1990–1996 (2006).

29. Pollack, A. *et al.* Dosimetry and preliminary acute toxicity in the first 100 men treated for prostate cancer on a randomized hypofractionation dose escalation trial. *Int. J. Radiat. Oncol. Biol. Phys.* **64**, 518–526 (2006).
30. Kupelian, P. A. *et al.* Radical prostatectomy, external beam radiotherapy < 72 Gy, external beam radiotherapy > or = 72 Gy, permanent seed implantation, or combined seeds/external beam radiotherapy for stage T1–T2 prostate cancer. *Int. J. Radiat. Oncol. Biol. Phys.* **58**, 25–33 (2004).  
**This retrospective analysis of nearly 3,000 patients illustrates that dose escalation can improve the outcome of radiotherapy, which might therefore become an alternative to surgery.**
31. Pow, E. H. *et al.* Xerostomia and quality of life after intensity-modulated radiotherapy vs. conventional radiotherapy for early-stage nasopharyngeal carcinoma: Initial report on a randomized controlled clinical trial. *Int. J. Radiat. Oncol. Biol. Phys.* **66**, 981–991 (2006).
32. De Ridder, M. *et al.* Phase II study of preoperative helical tomotherapy for rectal cancer. *Int. J. Radiat. Oncol. Biol. Phys.* (in press).
33. Emami, B. *et al.* Tolerance of normal tissue to therapeutic irradiation. *Int. J. Radiat. Oncol. Biol. Phys.* **21**, 109–122 (1991).
34. Tome, W. A. & Fowler, J. F. Selective boosting of tumor subvolumes. *Int. J. Radiat. Oncol. Biol. Phys.* **48**, 593–599 (2000).
35. Deasy, J. O. Partial tumor boosts: even more attractive than theory predicts? *Int. J. Radiat. Oncol. Biol. Phys.* **51**, 279–280 (2001).
36. Gambhir, S. S. Molecular imaging of cancer with positron emission tomography. *Nature Rev. Cancer* **2**, 683–693 (2002).
37. Payne, G. S. & Leach, M. O. Applications of magnetic resonance spectroscopy in radiotherapy treatment planning. *Br. J. Radiol.* **79**, S16–S26 (2006).
38. Thorwarth, D., Eschmann, S. M., Paulsen, F. & Alber, M. Hypoxia dose painting by numbers: a planning study. *Int. J. Radiat. Oncol. Biol. Phys.* **68**, 291–300 (2007).
39. Ling, C. C. *et al.* Towards multidimensional radiotherapy (MD-CRT): biological imaging and biological conformality. *Int. J. Radiat. Oncol. Biol. Phys.* **47**, 551–560 (2000).  
**This critical review summarizes the advances in imaging that have potential applications in radiation oncology, and explores the concept of integrating physical and biological conformality in CRT.**
40. Bentzen, S. M. Theragnostic imaging for radiation oncology: dose-painting by numbers. *Lancet Oncol.* **6**, 112–117 (2005).
41. Fletcher, G. H. Hypofractionation: lessons from complications. *Radiother. Oncol.* **20**, 10–15 (1991).
42. Harrison, D., Crennan, E., Cruickshank, D., Hughes, P. & Ball, D. Hypofractionation reduces the therapeutic ratio in early glottic carcinoma. *Int. J. Radiat. Oncol. Biol. Phys.* **15**, 365–372 (1988).
43. Kim, J. J. & Tannock, I. F. Repopulation of cancer cells during therapy: an important cause of treatment failure. *Nature Rev. Cancer* **5**, 516–525 (2005).
44. Herfarth, K. K. *et al.* Stereotactic single-dose radiation therapy of liver tumors: results of a phase I/II trial. *J. Clin. Oncol.* **19**, 164–170 (2001).
45. Nagata, Y. *et al.* Clinical outcomes of a phase I/II study of 48 Gy of stereotactic body radiotherapy in 4 fractions for primary lung cancer using a stereotactic body frame. *Int. J. Radiat. Oncol. Biol. Phys.* **63**, 1427–1431 (2005).
46. Xia, T. *et al.* Promising clinical outcome of stereotactic body radiation therapy for patients with inoperable Stage I/II non-small-cell lung cancer. *Int. J. Radiat. Oncol. Biol. Phys.* **66**, 117–125 (2006).
47. Haus, A. G., Pinsky, S. M. & Marks, J. E. A technique for imaging patient treatment area during a therapeutic radiation exposure. *Radiology* **97**, 653–656 (1970).
48. Marks, J. E. & Haus, A. G. The effect of immobilisation on localisation error in the radiotherapy of head and neck cancer. *Clin. Radiol.* **27**, 175–177 (1976).
49. Kinzie, J. J., Hanks, G. E., MacLean, C. J. & Kramer, S. Patterns of care study: Hodgkin's disease relapse rates and adequacy of portals. *Cancer* **52**, 2223–2226 (1983).  
**This can be considered as one of the first studies to correlate misalignment of treatment beams detected by daily imaging and recurrence.**
50. Rabinowitz, I., Broomberg, J., Goitein, M., McCarthy, K. & Leong, J. Accuracy of radiation field alignment in clinical practice. *Int. J. Radiat. Oncol. Biol. Phys.* **11**, 1857–1867 (1985).
51. Byhardt, R. W., Cox, J. D., Hornburg, A. & Liermann, G. Weekly localization films and detection of field placement errors. *Int. J. Radiat. Oncol. Biol. Phys.* **4**, 881–887 (1978).
52. Holloway, A. F. A localising device for a rotating cobalt therapy unit. *Br. J. Radiol.* **31**, 227 (1958).
53. Johns, H. E. & Cunningham, J. R. A precision cobalt 60 unit for fixed field and rotation therapy. *Am. J. Roentgenol. Radium. Ther. Nucl. Med.* **81**, 4–12 (1959).
54. Weissbluth, M., Karzmark, C. J., Steele, R. E. & Selby, A. H. The Stanford medical linear accelerator. II. Installation and physical measurements. *Radiology* **72**, 242–253 (1959).  
**References 52–54 illustrate some of the earlier attempts at improving image quality in the verification process of treatment by mounting X-ray devices on treatment machines. Many of more recent developments in IGRT are based on these concepts.**
55. Verhey, L. J., Goitein, M., McNulty, P., Munzenrider, J. E. & Suit, H. D. Precise positioning of patients for radiation therapy. *Int. J. Radiat. Oncol. Biol. Phys.* **8**, 289–294 (1982).
56. Leong, J. Use of digital fluoroscopy as an on-line verification device in radiation therapy. *Phys. Med. Biol.* **31**, 985–992 (1986).
57. De Neve, W. *et al.* Routine clinical on-line portal imaging followed by immediate field adjustment using a tele-controlled patient couch. *Radiother. Oncol.* **24**, 45–54 (1992).
58. Ezz, A. *et al.* Daily monitoring and correction of radiation field placement using a video-based portal imaging system: a pilot study. *Int. J. Radiat. Oncol. Biol. Phys.* **22**, 159–165 (1992).
59. Meertens, H., Van Herk, M. & Weeda, J. A liquid ionisation detector for digital radiography of therapeutic megavoltage photon beams. *Phys. Med. Biol.* **30**, 313–321 (1985).
60. Van Herk, M. & Meertens, H. A matrix ionisation chamber imaging device for on-line patient setup verification during radiotherapy. *Radiother. Oncol.* **11**, 369–378 (1988).
61. Herman, M. G. *et al.* Clinical use of electronic portal imaging: report of AAPM Radiation Therapy Committee Task Group 58. *Med. Phys.* **28**, 712–737 (2001).  
**Electronic portal imaging devices initiated the concept of IGRT as “in-room imaging during the course of treatment with decisions made based on this information”. The AAPM report TG 58 offers a nice overview of the different technical solutions, clinical use and quality assurance.**
62. Bel, A. *et al.* A computerized remote table control for fast on-line patient repositioning: implementation and clinical feasibility. *Med. Phys.* **27**, 354–358 (2000).
63. Jaffray, D. A., Siewerdsen, J. H., Wong, J. W. & Martinez, A. A. Flat-panel cone-beam computed tomography for image-guided radiation therapy. *Int. J. Radiat. Oncol. Biol. Phys.* **53**, 1337–1349 (2002).
64. Verellen, D. *et al.* Quality assurance of a system for improved target localization and patient set-up that combines real-time infrared tracking and stereoscopic X-ray imaging. *Radiother. Oncol.* **67**, 129–141 (2003).
65. Verellen, D. in *Image-guided IMRT: Concepts and Clinical Applications* (eds Bortfeld, T., Schmiidt-Ulrich, R. & De Neve, W.) (Springer-Verlag, Berlin, 2005).
66. Verellen, D., Soete, G., Linthout, N., Tournel, K. & Storme, G. Optimal control of set-up margins and internal margins for intra- and extracranial radiotherapy using stereoscopic kilovoltage imaging. *Cancer Radiother.* **10**, 235–244 (2006).
67. Soete, G., Verellen, D., Tournel, K. & Storme, G. Setup accuracy of stereoscopic X-ray positioning with automated correction for rotational errors in patients treated with conformal arc radiotherapy for prostate cancer. *Radiother. Oncol.* **80**, 371–373 (2006).
68. Linthout, N. *et al.* Assessment of secondary patient motion induced by automated couch movement during on-line 6 dimensional repositioning in prostate cancer treatment. *Radiother. Oncol.* **83**, 168–174 (2007).
69. Murphy, M. J. An automatic six-degree-of-freedom image registration algorithm for image-guided frameless stereotactic radiosurgery. *Med. Phys.* **24**, 857–866 (1997).
70. Shirato, H. *et al.* Four-dimensional treatment planning and fluoroscopic real-time tumor tracking radiotherapy for moving tumor. *Int. J. Radiat. Oncol. Biol. Phys.* **48**, 435–442 (2000).
71. Shirato, H. *et al.* Physical aspects of a real-time tumor tracking system for gated radiotherapy. *Int. J. Radiat. Oncol. Biol. Phys.* **48**, 1187–1195 (2000).
72. Murphy, M. J. *et al.* The effectiveness of breath-holding to stabilize lung and pancreas tumors during radiosurgery. *Int. J. Radiat. Oncol. Biol. Phys.* **53**, 475–482 (2002).
73. Verellen, D. *et al.* Importing measured field fluences into the treatment planning system to validate a breathing synchronized DMLC-IMRT irradiation technique. *Radiother. Oncol.* **78**, 332–338 (2006).
74. Verellen, D. *et al.* Breathing synchronized irradiation using stereoscopic KV-imaging to limit influence of interplay between leaf motion and organ motion in 3D-CRT and IMRT: Dosimetric verification and first clinical experience. *Int. J. Radiat. Oncol. Biol. Phys.* **66**, 108–119 (2006).
75. Lu, W., Parikh, P. J., Hubenschmidt, J. P., Bradley, J. D. & Low, D. A. A comparison between amplitude sorting and phase-angle sorting using external respiratory measurement for 4D CT. *Med. Phys.* **33**, 2964–2974 (2006).
76. Ford, E. C., Mageras, G. S., Yorke, E. & Ling, C. C. Respiration-correlated spiral CT: a method of measuring respiratory-induced anatomic motion for radiation treatment planning. *Med. Phys.* **30**, 88–97 (2003).
77. Hansen, V. N., Evans, P. M. & Swindell, W. The application of transit dosimetry to precision radiotherapy. *Med. Phys.* **23**, 713–721 (1996).
78. Pasma, K. L., Heijmen, B. J., Kroonwijk, M. & Visser, A. G. Portal dose image (PDI) prediction for dosimetric treatment verification in radiotherapy. I. An algorithm for open beams. *Med. Phys.* **25**, 830–840 (1998).
79. Mackie, T. R. *et al.* Image guidance for precise conformal radiotherapy. *Int. J. Radiat. Oncol. Biol. Phys.* **56**, 89–105 (2003).
80. Lof, J., Lind, B. K. & Brahme, A. An adaptive control algorithm for optimization of intensity modulated radiotherapy considering uncertainties in beam profiles, patient set-up and internal organ motion. *Phys. Med. Biol.* **43**, 1605–1628 (1998).
81. Brahme, A. Biologically optimized 3-dimensional *in vivo* predictive assay-based radiation therapy using positron emission tomography-computerized tomography imaging. *Acta Oncol.* **42**, 123–136 (2003).
82. Song, P. Y. *et al.* A comparison of four patient immobilization devices in the treatment of prostate cancer patients with three dimensional conformal radiotherapy. *Int. J. Radiat. Oncol. Biol. Phys.* **34**, 213–219 (1996).
83. Wulf, J., Hadinger, U., Oppitz, U., Olshausen, B. & Flentje, M. Stereotactic radiotherapy of extracranial targets: CT-simulation and accuracy of treatment in the stereotactic body frame. *Radiother. Oncol.* **57**, 225–236 (2000).
84. Hodge, W. *et al.* Feasibility report of image guided stereotactic body radiotherapy (IG-SBRT) with tomotherapy for early stage medically inoperable lung cancer using extreme hypofractionation. *Acta Oncol.* **45**, 890–896 (2006).
85. Van Herk, M., Remeijer, P. & Lebesque, J. V. Inclusion of geometric uncertainties in treatment plan evaluation. *Int. J. Radiat. Oncol. Biol. Phys.* **52**, 1407–1422 (2002).
86. Zhang, L. *et al.* Multiple regions-of-interest analysis of setup uncertainties for head-and-neck cancer radiotherapy. *Int. J. Radiat. Oncol. Biol. Phys.* **64**, 1559–1569 (2006).
87. Polat, B., Wilbert, J., Baier, K., Flentje, M. & Guckenberger, M. Nonrigid patient setup errors in the head-and-neck region. *Strahlenther. Onkol.* **183**, 506–511 (2007).
88. Kashani, R., Hub, M., Kessler, M. L. & Balter, J. M. Technical note: a physical phantom for assessment of accuracy of deformable alignment algorithms. *Med. Phys.* **34**, 2785–2788 (2007).
89. Murphy, M. *et al.* The management of imaging dose during image-guided radiotherapy: Report of the AAPM Task Group 75. *Med. Phys.* **34**, 4041–4063. (2007).
90. Biggs, P. J., Goitein, M. & Russell, M. D. A diagnostic X-ray field verification device for a 10 MV linear accelerator. *Int. J. Radiat. Oncol. Biol. Phys.* **11**, 635–643 (1985).
91. Shiu, A. S., Hogstrom, K. R., Janjan, N. A., Fields, R. S. & Peters, L. J. Technique for verifying treatment fields using portal images with diagnostic quality. *Int. J. Radiat. Oncol. Biol. Phys.* **13**, 1589–1594 (1987).
92. Munro, P. & Bouiuis, D. C. X-ray quantum limited portal imaging using amorphous silicon flat-panel arrays. *Med. Phys.* **25**, 689–702 (1998).
93. Guckenberger, M. *et al.* Precision of image-guided radiotherapy (IGRT) in six degrees of freedom and limitations in clinical practice. *Strahlenther. Onkol.* **183**, 307–313 (2007).

94. Murphy, M. J. *et al.* Image-guided radiosurgery for the spine and pancreas. *Comput. Aided Surg.* **5**, 278–288. (2000).
95. Aoki, Y. *et al.* An integrated radiotherapy treatment system and its clinical application. *Radiat. Med.* **5**, 131–141 (1987).
96. Court, L., Rosen, I., Mohan, R. & Dong, L. Evaluation of mechanical precision and alignment uncertainties for an integrated CT/LINAC system. *Med. Phys.* **30**, 1198–1210 (2003).
97. Kuriyama, K. *et al.* A new irradiation unit constructed of self-moving gantry-CT and linac. *Int. J. Radiat. Oncol. Biol. Phys.* **55**, 428–435 (2003).
98. Uematsu, M. *et al.* Intrafractional tumor position stability during computed tomography (CT)-guided frameless stereotactic radiation therapy for lung or liver cancers with a fusion of CT and linear accelerator (FOCAL) unit. *Int. J. Radiat. Oncol. Biol. Phys.* **48**, 443–448 (2000).
99. Holupka, E. J., Kaplan, I. D., Burdette, E. C. & Svensson, G. K. Ultrasound image fusion for external beam radiotherapy for prostate cancer. *Int. J. Radiat. Oncol. Biol. Phys.* **35**, 975–984 (1996).
100. Lattanzi, J. *et al.* A comparison of daily CT localization to a daily ultrasound-based system in prostate cancer. *Int. J. Radiat. Oncol. Biol. Phys.* **43**, 719–725 (1999).
101. Langen, K. M. *et al.* Evaluation of ultrasound-based prostate localization for image-guided radiotherapy. *Int. J. Radiat. Oncol. Biol. Phys.* **57**, 635–644 (2003).
102. Van den Heuvel, F. *et al.* Independent verification of ultrasound based image-guided radiation treatment, using electronic portal imaging and implanted gold markers. *Med. Phys.* **30**, 2878–2887 (2003).
103. Seiler, P. G., Blattmann, H., Kirsch, S., Muench, R. K. & Schilling, C. A novel tracking technique for the continuous precise measurement of tumour positions in conformal radiotherapy. *Phys. Med. Biol.* **45**, N103–N110 (2000).
104. Litzenberg, D. W. *et al.* Positional stability of electromagnetic transponders used for prostate localization and continuous, real-time tracking. *Int. J. Radiat. Oncol. Biol. Phys.* **68**, 1199–1206 (2007).
105. Takai, Y., Mitsuya, M. & Nemoto, K. Development of a new linear accelerator mounted with dual X-ray fluoroscopy using amorphous silicon flat panel X-ray sensors to detect a gold seed in a tumor at real treatment position. *Int. J. Radiat. Oncol. Biol. Phys.* **51**, 381 (2001).
106. Pouliot, J. *et al.* Low-dose megavoltage cone-beam CT for radiation therapy. *Int. J. Radiat. Oncol. Biol. Phys.* **61**, 552–560 (2005).
107. Mackie, T. R. *et al.* Tomotherapy: a new concept for the delivery of dynamic conformal radiotherapy. *Med. Phys.* **20**, 1709–1719 (1993).
108. Fenwick, J. D. *et al.* Quality assurance of a helical tomotherapy machine. *Phys. Med. Biol.* **49**, 2933–2953 (2004).
109. Carol, M. Peacock: a system for planning and rotational delivery of intensity-modulated fields. *Int. J. Imag. Syst. Technol.* **6**, 56–61 (1995).
110. Verellen, D., Linthout, N., Van den, B. D., Bel, A. & Storme, G. Initial experience with intensity-modulated conformal radiation therapy for treatment of the head and neck region. *Int. J. Radiat. Oncol. Biol. Phys.* **39**, 99–114 (1997).
111. Verellen, D., Linthout, N. & Storme, G. Target localization and treatment verification for intensity modulated conformal radiation therapy of the head and neck region. *Strahlenther. Onkol.* **174**, 19–27 (1998).
112. Kamino, Y. *et al.* Development of a four-dimensional image-guided radiotherapy system with a gimbaled X-ray head. *Int. J. Radiat. Oncol. Biol. Phys.* **66**, 271–278 (2006).
113. Raaijmakers, A. J., Raaymakers, B. W., van der, M. S. & Lagendijk, J. J. Integrating a MRI scanner with a 6 MV radiotherapy accelerator: impact of the surface orientation on the entrance and exit dose due to the transverse magnetic field. *Phys. Med. Biol.* **52**, 929–939 (2007).
114. Janek, S., Svensson, R., Jonsson, C. & Brahme, A. Development of dose delivery verification by PET imaging of photonuclear reactions following high energy photon therapy. *Phys. Med. Biol.* **51**, 5769–5783 (2006).
115. Langen, K. M. & Jones, D. T. Organ motion and its management. *Int. J. Radiat. Oncol. Biol. Phys.* **50**, 265–278 (2001).
- The authors compiled and reviewed existing data on inter- and intra-fraction motion of different organs and tumours, and discussed some of the techniques that can be used to manage this motion in radiotherapy.**
116. Lax, I., Blomgren, H., Naslund, I. & Svanstrom, R. Stereotactic radiotherapy of malignancies in the abdomen. Methodological aspects. *Acta Oncol.* **33**, 677–683 (1994).
117. Wong, J. W. *et al.* The use of active breathing control (ABC) to reduce margin for breathing motion. *Int. J. Radiat. Oncol. Biol. Phys.* **44**, 911–919 (1999).
118. Mah, D. *et al.* Technical aspects of the deep inspiration breath-hold technique in the treatment of thoracic cancer. *Int. J. Radiat. Oncol. Biol. Phys.* **48**, 1175–1185 (2000).
119. Caldwell, C. B., Mah, K., Skinner, M. & Danjoux, C. E. Can PET provide the 3D extent of tumor motion for individualized internal target volumes? A phantom study of the limitations of CT and the promise of PET. *Int. J. Radiat. Oncol. Biol. Phys.* **55**, 1381–1393 (2003).
120. Ohara, K. *et al.* Irradiation synchronized with respiration gate. *Int. J. Radiat. Oncol. Biol. Phys.* **17**, 853–857 (1989).
121. Keall, P. J., Kini, V. R., Vedam, S. S. & Mohan, R. Motion adaptive x-ray therapy: a feasibility study. *Phys. Med. Biol.* **46**, 1–10 (2001).
122. Brock, K. K. *et al.* Inclusion of organ deformation in dose calculations. *Med. Phys.* **30**, 290–295 (2003).
123. Bortfeld, T., Jiang, S. B. & Rietzel, E. Effects of motion on the total dose distribution. *Semin. Radiat. Oncol.* **14**, 41–51 (2004).
124. Guckenberger, M. *et al.* Four-dimensional treatment planning for stereotactic body radiotherapy. *Int. J. Radiat. Oncol. Biol. Phys.* **69**, 276–285 (2007).
125. Bosmans, G. *et al.* An “*in silico*” clinical trial comparing free breathing, slow and respiration correlated computed tomography in lung cancer patients. *Radiother. Oncol.* **81**, 73–80 (2006).
126. Faria, S. *et al.* Radiotherapy volume delineation with PET in lung cancer may be less useful than foreseen. *J. Thorac. Oncol.* **2**, 347–348 (2007).
127. Lagerwaard, F. J. *et al.* Multiple ‘slow’ CT scans for incorporating lung tumor mobility in radiotherapy planning. *Int. J. Radiat. Oncol. Biol. Phys.* **51**, 932–937 (2001).
128. Jiang, S. B. *et al.* An experimental investigation on intra-fractional organ motion effects in lung IMRT treatments. *Phys. Med. Biol.* **48**, 1773–1784 (2003).
129. de Mey, J. *et al.* Percutaneous placement of marking coils before stereotactic radiation therapy of malignant lung lesions. *J. Vasc. Interv. Radiol.* **16**, 51–56 (2005).
130. Schweikard, A., Glosner, G., Bodduluri, M., Murphy, M. J. & Adler, J. R. Robotic motion compensation for respiratory movement during radiosurgery. *Comput. Aided Surg.* **5**, 263–277 (2000).
131. Mageras, G. S. *et al.* Fluoroscopic evaluation of diaphragmatic motion reduction with a respiratory gated radiotherapy system. *J. Appl. Clin. Med. Phys.* **2**, 191–200 (2001).
132. Hanley, J. *et al.* Deep inspiration breath-hold technique for lung tumors: the potential value of target immobilization and reduced lung density in dose escalation. *Int. J. Radiat. Oncol. Biol. Phys.* **45**, 603–611 (1999).
133. Murphy, M. J. Tracking moving organs in real time. *Semin. Radiat. Oncol.* **14**, 91–100 (2004).
134. Keall, P. J. *et al.* The management of respiratory motion in radiation oncology report of AAPM Task Group 76. *Med. Phys.* **33**, 3874–3900 (2006).
- This report describes observed magnitudes of respiratory motion, discusses specific problems related to radiotherapy, explains techniques to manage respiratory motion and gives recommendations in the applications of these techniques for patient care.**
135. Suit, H. D. in Proc. Conf. Time Dose Relationships Radiat. Biol. Applied Radiother. (Brookhaven National Laboratory, New York, 1970).

## DATABASES

Entrez Gene: <http://www.ncbi.nlm.nih.gov/entrez/query.fcgi?db=gene>  
 EGF | VEGF  
 National Cancer Institute: <http://www.cancer.gov/head-and-neck-cancer> | [hepatic malignancies](http://www.cancer.gov/hepatic-malignancies) | [Hodgkin disease](http://www.cancer.gov/hodgkin-disease) | [pancreatic cancer](http://www.cancer.gov/pancreatic-cancer) | [prostate cancer](http://www.cancer.gov/prostate-cancer) | [rectal cancer](http://www.cancer.gov/rectal-cancer)

ALL LINKS ARE ACTIVE IN THE ONLINE PDF

---

**ERRATUM**

## Innovations in image-guided radiotherapy

*Dirk Verellen, Mark De Ridder, Nadine Linthout, Koen Tournel, Guy Soete and Guy Storme*

*Nature Reviews Cancer* **7**, 949–960 (2007)

There is an error in Box 1 of this article on page 951. The formula for the volume of a sphere is incorrectly shown; it should read  $\frac{4}{3}\pi r^3$ . This has been corrected online.